HYPERELASTIC CONSTITUTIVE MODELLING FOR 3D TEXTILE REINFORCEMENTS: FROM OBSERVATION TO MODELING

A. Charmetant[1], E. Vidal-Sallé[1*], P. Boisse[1]

[1]*(LaMCoS) INSA Lyon, UMR CNRS 52 59, Université de Lyon, France*
**emmanuelle.vidal-salle@insa-lyon.fr*

Keywords: hyperelasticity, interlock, constitutive modeling, finite element

Abstract
The present paper deals with the hyperelastic approach to model the constitutive behavior of dry fabric reinforcement for structural composites. The proposed approach, based on experimental observations, assumes uncoupling between several deformation modes. The paper presents also the identification procedure and some examples show the ability of the proposed method to describe the deformation of 3D thick interlock fabrics.

1 Introduction

For critical structural parts where in-use delamination has to be strictly avoided, composites using 3D thick interlock reinforcements represent a promising alternative to metallic alloys [1]. Generally, structural parts built with those composites are produced using Resin Transfer Molding processes [2;3]. The first stage of that process consists in forming the dry reinforcement. If the forming of metallic parts is well known, it is not really the case for those thick reinforcements. For several years, various numerical techniques have been developed to simulate the forming stage of the RTM processes for thin reinforcements [4-9]. For thick interlock reinforcements, there are few proposals [10]. Like for 2D reinforcements, 3D ones present a behavior which is highly influenced by the yarn orientation and density. That means that the meso- and micro- structures must be taken into account even for a 3D macroscopic modeling.

The first stage of an efficient modeling passes through the identification of the effective deformation modes which can be observed for such structure (seen as a material). Such identification is the topic of the first part of the present contribution.

When a material has to be described, several approaches are possible: elastic, hypo-elastic or hyper-elastic. The second part of the paper presents the drawbacks and advantages of hypo- and hyper- elastic approaches and presents the general framework of hyper-elasticity.

Then the approach is explained for the mesoscopic level. The macroscopic one is an extension of the previous meso- one. In order to achieve the implementation of the constitutive equation, several strain invariants are defined, which are representative to each deformation mode. The identification procedure is described and first results show the capability of the proposed approach to describe accurately the forming of dry reinforcements for structural composite parts.

2 Textile material and deformation modes

2.1 Yarn architecture

A thick interlock material is built by the assembly of a large number of yarns (see figure 1), each yarn being made up of thousands of individual fibers. Generally, flat preforms, because they are realized using classical weaving looms present two main orientations (warp and weft) which are approximately orthogonal, so that the fabric can generally be considered as initially orthotropic.

Looking at the lower scale, the orientation of the fibers inside the fiber bundle is more or less unidirectional with a quasi-isotropic distribution of the fibers inside the bundle which generally leads to consider the yarn as a transversely isotropic material.

Based on those considerations, one can admit that a thick interlock fabric is a generalization of a single yarn structure for which there are two fiber directions instead of a single one. During the forming operation, the initially orthogonal yarn directions will rotate with a large amplitude so that the material will not remain orthotropic to become anisotropic.

Figure 1. thick interlock (a) and the tomography of a single yarn (b)

In order make the explanations clearer, the following will be done on the single yarn, the extension for thick interlock material being done later.

2.2 Yarn deformation modes

Because the yarn is not really continuous, the deformation modes of what will be called later the "yarn material" are not exactly the same as the deformation modes classically observed in continuous media: some of them disappear or can be neglected. For a transversely isotropic material, four deformation modes are considered: the elongation along the fiber direction; the shear along the fiber direction; considering the "section" perpendicular to the longitudinal direction (the isotropy plan) the compaction and; the shear in the isotropy plane (see figure 2).

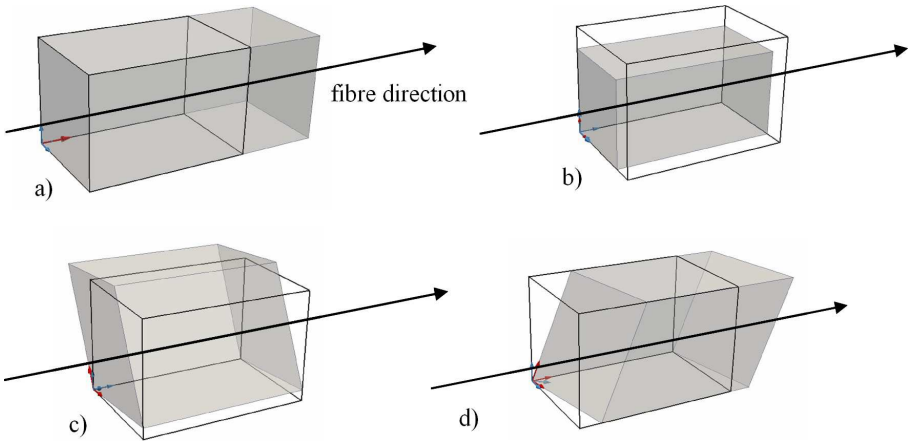

Figure 2. Deformation modes of the yarn: (a) elongation (b) compaction of the cross section (c) distortion of the cross section (d) longitudinal shear

2.3 Uncoupling assumptions

Previous works have shown that coupling exists between the behaviors corresponding to the deformation modes defined above [11]. In particular the fiber density, which depends on the compaction, is an important parameter to describe all the other yarn mechanical behaviors. The proposed model does not take these couplings into account.

3. Hyper-elasticity vs hypo-elasticity

As mentioned in the introduction, finite element simulations for dry fabric modeling generally use hypo-elastic constitutive equations for both meso- and macro- scale modeling [12;8]. The main advantage to use hypo-elastic models is that they are classically implemented for plasticity simulation, which reduces the modeling effort. Such approach leads to define an objective derivative of the Cauchy stress tensor as a function of the strain rate tensor (eq 1).

$$\underline{\underline{\sigma}}^{\nabla} = \underline{\underline{\underline{\underline{C}}}} : \underline{\underline{D}} \tag{1}$$

The main drawback of such models leads in the difficulty to choose an adequate time derivative of the stress tensor. It has been shown [13] that for strongly anisotropic materials like yarns or fabrics, the only consistent derivative is the one which guaranties a correct following of the fiber direction which requires a strict follow-up of such direction.

In the case of two fiber directions, as they do not remain perpendicular during the forming process, it implies either to work on non orthogonal frames [14], or on two different frames [8] and then, realize the superimposition of the contributions of both networks for each time increment. Neither of those solutions is easy to implement in standard finite element codes.

Hyper-elastic approaches are generally written in the Lagrangian initial configuration for which the working frame is already orthogonal which avoids the difficult follow up of the current fiber directions. In order to define a hyperelastic material, an elastic strain energy potential per unit volume w must exist which only depends on the current strain state. Derivating that strain energy density function with regard to the right Cauchy Green strain tensor components, one can evaluate the second Piola-Kirchhoff stress tensor components:

$$\underline{\underline{S}} = 2\frac{\partial w}{\partial \underline{\underline{C}}} \tag{2}$$

In order to ensure that this constitutive equation fulfils the principle of material frame indifference, function w must be written as a function of invariants of the right Cauchy Green deformation tensor $\underline{\underline{C}}$. It must satisfy the principle of material symmetry, i.e. the strain energy must be invariant under any transformation belonging to the symmetry group of the material. It has been shown [15] that an isotropic function $\tilde{w}$ exists which depends on the right Cauchy-Green strain tensor $\underline{\underline{C}}$ and structural tensors $\underline{\underline{\underline{\underline{G}}}}_i$ defining the symmetry group, such as:

$$\underline{\underline{\underline{\underline{G}}}}_i = \underline{G}_i \otimes \underline{G}_i \tag{3}$$

where $\underline{G}_i$ are the initial fiber directions.

It has been shown [16] that for transversely isotropic materials, the number of strain and structural invariants required is equal to five:

$$I_1 = Tr\left(\underline{\underline{C}}\right) \quad I_2 = \frac{1}{2}\left(Tr\left(\underline{\underline{C}}\right)^2 - Tr\left(\underline{\underline{C}}^2\right)\right) \quad I_3 = Det\left(\underline{\underline{C}}\right)$$
$$I_4 = \underline{G}_1 \cdot \underline{\underline{C}} \cdot \underline{G}_1 \qquad I_5 = \underline{G}_1 \cdot \underline{\underline{C}}^2 \cdot \underline{G}_1 \tag{4}$$

I_1 to I_3 are the classical strain invariants and I_4 and I_5 are called mixed invariants.
The main drawback of hyper-elastic models is inherent to the difficulty to easily build coupled models and to introduce dissipative behaviors. But, for 2D thin fabrics, an uncoupled model [17] has shown its ability to describe accurately the membrane behavior of a thin fabric because the identification of the strain energy density function is done using experimental results taking implicitly into account those couplings.

4. Hyper-elastic constitutive model for yarn material

4.1 Physically based invariants

It has been shown in section 2 that four deformation modes can be identified and five strain invariants must be used to define the strain energy density function from which the constitutive behavior must derive. There are two ways to define those invariants. The methodology exposed in [18] leads to results very similar to the ones presented here.
If vector $\underline{G}_1$ is a unit vector along the fiber direction, the elongation of the yarn in the direction of fibers is directly given by invariant I_4 defined in (eq. 4). Consequently, this quantity can be chosen as the representative value of the length change of the yarn:

$$I_{elong} = I_4 \tag{5}$$

Yarn compaction can be defined as the ratio between the volume change and the length change of the yarn:

$$I_{comp} = \sqrt{\frac{I_3}{I_4}} \tag{6}$$

when distortion and transverse shear have expression a little more complicated and use the other strain and structural invariants defined in (eq. 4) [18]:

$$I_{dist} = \sqrt{I_1 - \frac{I_5}{I_4} - 2\sqrt{\frac{I_3}{I_4}}} \text{ and } I_{cis} = \sqrt{\frac{I_5}{I_4} - I_4} \tag{7}$$

4.2 Strain energy density function shape and parameter identification

Due to the abovementioned uncoupling assumption, the constitutive equation can be written as a summation of four strain energy density functions representative to each deformation mode.

$$w = w_{elong}\left(I_{elong}\right) + w_{comp}\left(I_{comp}\right) + w_{dist}\left(I_{dist}\right) + w_{cis}\left(I_{cis}\right) \tag{8}$$

The second Piola-Kirchhoff stress tensor is calculated by the derivative of such sum:

$$\underline{\underline{S}} = 2\frac{\partial w}{\partial \underline{\underline{C}}} = 2\left(\frac{\partial w_{elong}}{\partial I_{elong}} \frac{\partial I_{elong}}{\partial \underline{\underline{C}}} + \frac{\partial w_{comp}}{\partial I_{comp}} \frac{\partial I_{comp}}{\partial \underline{\underline{C}}} + \frac{\partial w_{dist}}{\partial I_{dist}} \frac{\partial I_{dist}}{\partial \underline{\underline{C}}} + \frac{\partial w_{cis}}{\partial I_{cis}} \frac{\partial I_{cis}}{\partial \underline{\underline{C}}} \right) \tag{9}$$

More details on the strain energy density function can be found in [18], the results are summarized here after.

4.2.1 Elongation along the fiber direction

The strain energy density function corresponding to the first straining mode, namely the longitudinal stretch, can be identified using a tensile test on a single yarn. In order to take into account the slight initial non linearity of the stretch curve, a piecewise function is chosen:

$$\begin{aligned} &\text{if } I_{elong} \le I_{elong0} \qquad w^{nl}_{elong}\left(I_{elong}\right) = a_0 + a_1\left(I_{elong}-1\right) + a_2\left(I_{elong}-1\right)^2 + a_3\left(I_{elong}-1\right)^3 \\ &\text{if } I_{elong} > I_{elong0} \qquad w^{lin}_{elong}\left(I_{elong}\right) = b_0 + b_1\left(I_{elong}-1\right) + b_2\left(I_{elong}-1\right)^2 \end{aligned} \tag{10}$$

4.2.2 Compaction and shape change of the cross section

The strain energy associated to the compaction and the distortion of the yarn transverse section is linked to several physical phenomena at the microscopic scale like rearrangement of fibers which are difficult to study separately. A power-based strain energy function is proposed for both compaction and distortion:

$$w_{comp}\left(I_{comp}\right) = K_{comp}\left(1-I_{comp}\right)^p \text{ and } w_{dist}\left(I_{dist}\right) = \frac{1}{2}K_{dist}{I_{dist}}^2 \tag{11}$$

The corresponding parameters can be identified using an equi-biaxial tensile test. Unfortunately, the solution is not unique and an optimization procedure like Levenberg-Marcquard one has to be used to evaluate the best set of parameters.

4.2.3 Transverse shear

The transverse shear strain energy of the yarn is linked to the sliding of its constitutive fibers in their preferred direction. Such a type of strain is basically dissipative as it is linked to friction. Nevertheless, the very small energies involved (as compared with the tensile strain energy in the longitudinal direction) allow assuming also for such straining mode, an elastic behavior. It is also assumed that the corresponding stiffness is constant which leads to a strain energy potential for the longitudinal shear such as:

$$w_{cis}\left(I_{cis}\right) = \frac{1}{2}K_{cis}{I_{cis}}^2 \tag{12}$$

A bending test allows the identification of such parameters.

5. Extension to 3D thick interlock fabrics

As mentioned in the introduction, a thick interlock fabric can be seen as an extension of the 3D yarn material behavior with two initially orthogonal fiber directions.

In such a case, it has been proved [19] that the number of strain invariants necessary to build a mathematically isotropic function raises up to eleven so that the strain energy density function can be written such as:

$$w^{orth} = w^{orth}\left(I_1, I_2, I_3, I_{41}, I_{42}, I_{43}, I_{412}, I_{423}, I_{51}, I_{52}, I_{53}\right) \tag{13}$$

with I_1 to I_3 the classical strain invariants defined in (4) and the eight other invariants defined such as:

$$I_{4i} = \underline{G}_i \cdot \underline{\underline{C}} \cdot \underline{G}_i \,,\; I_{4ij} = \underline{G}_i \cdot \underline{\underline{C}} \cdot \underline{G}_j \text{ and } I_{5i} = \underline{G}_i \cdot \underline{\underline{C}}^2 \cdot \underline{G}_i \;\; (i = 1,3) \tag{14}$$

5.1 Deformation modes

In a 3D case for thick interlocks, the number of elementary deformation modes raises up to six as shown in figure 3.

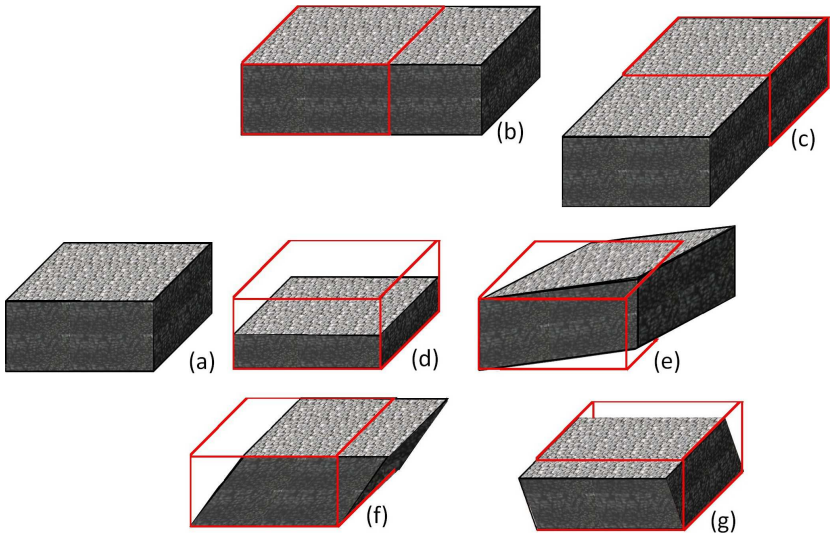

Figure 3. Deformation modes of a thick interlock: (a) undeformed shape; (b) and (c) stretches in warp and weft direction; (d) transverse compression, (e) in-plane shear, (f) and (g) transverse shear along warp and weft.

5.2 Potentialities of the model

The identification procedure is very similar to the one used for the mesoscopic modeling. It uses uniaxial tensile tests on warp and weft directions, in-plane shear and transverse shear along warp and weft directions, and finally transverse compaction.

Both meso- and macro- scopic models have been implemented in ABAQUS/Explicit finite element code and allow comparing experimental and numerical forming simulations.

6. Conclusion and future works

A constitutive equation based on a phenomenological approach has been proposed for both meso- and macro- scale textile modeling. Both are based on the definition of physically based strain invariants able to describe the elementary deformation modes of textile materials and accounting for the material orientation.

A strong assumption of uncoupling between all modes is done. Despite this non realistic assumption, both models prove their ability to describe in a reasonable accuracy, the behavior of such kind of materials because the identification procedure implicitly takes those couplings into account. Following this assumption, the strain energy density function can be built as the addition of strain energy density functions depending on a single strain invariant, each invariant being representative of the corresponding deformation mode. The total stress state is then obtained by the addition of all the contributions.

An identification procedure is proposed based on classical mechanical tests for fabrics such as uni- and bi- axial tensile tests, in-plane shear tests (like picture frame test or bias extension tests), and bending tests.

Some forming simulations have been preformed and show a pretty good agreement with experimental evidences.
In order to show the robustness of the approach it is necessary to use the same yarn material with various weaving patterns (for the mesoscale model) and to realize new experimental forming on the same thick interlock where all the deformation modes are activated.

Acknowledgents
The support of SNECMA company (Groupe SAFRAN) is gratefully acknowledged.

References
[1] Mouritz AP, Bannister MK, Falzon PJ, Leong KH, Review of applications for advanced three-dimensional fibre textile composites. *Composites Part A* **30**: 1445–1461 (1999).
[2] Rudd, C.D. and Long, A.C. *Liquid molding technologies*, Woodhead Publishing Limited (1997).
[3] Parnas, R.S. *Liquid composite molding*, Hanser, Garner Publications. (2000).
[4] Van Der Weën, F. Algorithms for Draping Fabrics on Double-curved Surfaces, *International Journal for Numerical Methods in Engineering* **31**: 1415-1426. (1991).
[5] Creech, G., Pickett, A.K. Meso-modelling of Non-Crimp Fabric composites for coupled drape and failure analysis, *Journal of Material Sciences* **41**: 6725-6736 (2006).
[6] Ben Boubaker, B., Haussy, B. and Ganghoffer, J.F. Discrete Models of Woven Structures. Macroscopic Approach, *Composites: Part B* **38(4)**: 498-505 (2007).
[7] Gatouillat S., Vidal-Sallé E., Boisse P. Advantages of the Meso/Macro Approach for the Simulation of Fibre Composite Reinforcements Int. *J. of Material Forming* **3 suppl. 1**: 643-646 (2010).
[8] Khan M.A., Mabrouki T., Vidal-Sallé E., Boisse P. Numerical and experimental analyses of woven composite reinforcement forming using a hypoelastic behaviour. Application to the double dome benchmark. *Journal of Materials Processing Technology* **210**: 378–388 (2010).
[9] Hamila N., Boisse P. Simulations of textile composite reinforcement draping using a new semi-discrete three node finite element. *Composites: Part B* **39**: 999–1010 (2008).
[10] De Luycker E., Morestin F., Boisse P., Marsal D. Simulation of 3D interlock composite performing *Composite Structures* **88**: 615–623 (2009).
[11] Buet–Gautier K., Boisse P. Experimental analysis and modeling of biaxial mechanical behavior of woven composite reinforcements. *Experimental Mechanics* **41**: 260–269 (2001).
[12] Badel, P., Vidal-Sallé, E., Maire, E. and Boisse, P. Simulation and tomography analysis of textile composite reinforcement deformation at the mesoscopic scale, *Composites Science and Technology* **68**: 2433–2440 (2008).
[13] Badel P., Vidal-Sallé E., Boisse P. Computational determination of in-plane shear mechanical behaviour of textile composite reinforcements *Computational Materials Science* **40**: 439–448 (2007).
[14] Hagège B. Simulation du comportement mécanique des milieux fibreux en grandes transformations. *PhD thesis ENSAM Paris* 263 p. (2004)
[15] Zheng, Q.S. Theory of representations for tensor functions – A unified invariant approach to constitutive equations, *Applied Mechanics Reviews* **47(11)**: 545–586 (1994).
[16] Criscione, J.C., Douglas, A.S. and Hunter, W.C. Physically based strain invariant set for materials exhibiting transversely isotropic behaviour *Journal of the Mechanics and Physics of Solids* **49**: 871–897 (2001).

[17] Aimène Y., Vidal–Sallé E., Hagège B., Sidoroff F., Boisse P. A hyperelastic approach for composite reinforcement large deformation analysis. *Journal of Composite Materials* **44 (1)**: 5–26 (2010).
[18] Charmetant A., Vidal-Sallé E., Boisse P. Hyperelastic modelling for mesoscopic analyses of composite reinforcements *Composites Science and Technology* **71**: 1623–1631 (2011).
[19] Ogden, R.W. *Non-linear Elastic Deformations*, Wiley and Sons, New York (1984).